ARTICLE

Absorption Spectrum of Neutral Krypton in the Near Infrared Region

Ruo-yu Jiang, Jia Ye, Lun-hua Deng*, Hai-ling Wang*

State Key Laboratory of Precision Spectroscopy, East China Normal University, Shanghai 200062, China

(Dated: Received on May 7, 2019; Accepted on June 15, 2019)

High-resolution absorption spectra of atomic krypton in the range of 11870−12700 cm^{-1} were recorded by employing concentration modulation absorption spectroscopy technique with a tunable single-mode cw Ti:Sapphire laser. The krypton atoms were excited to the absorbing energy states by discharge-burning in a mixture of helium and krypton. A total of 120 lines of neutral krypton were observed, among them 33 lines have already been classified in previous studies, 45 lines were newly classified with the known energy levels, and 42 lines cannot be classified. These unclassified lines indicate that up to now unknown energy levels of Kr must exist. Further, an analysis of the unclassified lines to get possible new energy levels with a classification program is reported.

Key words: Neutral krypton, Absorption Spectrum, Energy levels

I. INTRODUCTION

The spectrum of neutral krypton has been the subject of many investigations for its wide variety of applications. It is commonly used in astrophysics, plasma physics and laser physics. For example, krypton is one of the most abundant elements with Z larger than 32 in the observations of Planetary Nebulae spectra [1], and it also has been detected in the spectra of the interstellar medium [2].

The spectrum of neutral krypton has been studied for decades, ranging from far ultraviolet to infrared. Meggers *et al.* [3, 4] investigated first the neutral spectra of krypton, and observed 460 spectral lines ranging from 3302 Å to 9751 Å. In 1933, Meggers and Humphreys [5] made further investigation and found 200 lines in the range of 7601 Å to 12124 Å. In 1949, Sittner and Peck [6] reported observations of neutral krypton lines between 1.2 and 2.2 μm, and three-fourths of these lines were classified with the known energy levels. In 1952, Humphreys *et al.* [7] investigated the spectra of Kr I in the infrared region from 12000 Å to 19000 Å, and reported 36 new lines of Kr I compared with the observations of Sittner and Peck [6]. In 1952, Moore [8] first compiled the energy levels of Kr I, and published the results in "atomic energy levels". In 1969, Kaufman and Humphreys [9] reported 530 lines of Kr I in the region of 3300−40700 Å, and determined 45 even-parity and 66 odd-parity levels of neutral ^{86}Kr. Jackson [10, 11] measured wavenumber shifts between pairs of the five stable even isotopes of Kr in fifteen 5s-5p lines, six 5s-6p lines, and one 5p-5d line. In 1989, Trickl *et al.* [12] measured the hyperfine structures and isotope shifts of the resonance lines of ^{86}Kr from four levels of the $4p^5$5s, 6s, 7s configurations under an average uncertainty of 1 part in 10^7. In 1991, Sugar and Musgrove [13] compiled the energy levels of Kr I considering the correction given by Trickl *et al.* [12]. In 2002, Sansonetti *et al.* [14] made high-resolution observations of Kr and other noble gases in the region of 0.7 μm to 5.0 μm. In 2007, combining all the available experimental data of observed spectral lines of krypton atom [15−25], Saloman [26] compiled the energy levels and the observed spectral lines of Kr I. In the same year, Sansonetti *et al.* [27] investigated the spectra of Kr I covering the region from 6699 Å to 12200 Å with a resolution of 0.01 cm^{-1}, and the region from 9000 Å to 47782 Å with a resolution of 0.007 cm^{-1}. They obtained 630 classified lines and among them 290 were newly observed.

In this work, we report the observation of a total of 120 spectral lines of Kr I in the region 7874−8425 Å (11870−12700 cm^{-1}). Among them 33 lines have been classified in previous studies, and 88 lines are newly observed in this work. The new lines include 45 lines which can be classified with the known energy levels and 42 lines which cannot be classified with the reported energy levels. The 42 unclassified lines indicate that there should exist up to now unknown energy levels of Kr I which have not been obtained in previous studies. As a result, we analyzed these new lines, and tried to get the new energy levels. However, we cannot give definite values for these possible new energy levels due to the larger Doppler width of our measured spectra of Kr. A new experiment in which well-separated hyperfine components can be observed is needed.

*Authors to whom correspondence should be addressed. E-mail: lhdeng@phy.ecnu.edu, hlwang@phy.ecnu.edu.cn

DOI:10.1063/1674-0068/cjcp1905089

II. EXPERIMENTS

This work utilizes the same experimental approach as for the former investigation of Bromine described in Ref.[28]. A tunable single-mode cw Ti:Sapphire laser (Coherent Ring 899-29) is operated in the region from 11870 cm^{-1} to 12700 cm^{-1} as the source of laser radiation. The main target cell is cylindrical in shape, 600 mm in length and 12 mm in diameter, which is filled with approximately 10 Pa of krypton gas and 100 Pa helium gas. A pair of cooper sheets is used as discharge electrodes, and a 23 kHz alternating current discharge in the target cell is used to generate the excited Kr atoms. Concentration modulation spectroscopy is applied to obtain the high-resolution spectrum of neutral Kr atoms. The spectrum of Kr is obtained by demodulating the signal from a detector at the doubled discharge frequency. The observed spectral line shape is a Gaussian profile with a line width of about 1 GHz. The laser wavenumber is recorded by an attached wavemeter with a resolution of 0.001 cm^{-1} and is further calibrated using results in Ref.[27]. The absolute accuracy of observed line positions is expected to be 0.002 cm^{-1}.

III. RESULTS AND DISCUSSION

Natural krypton is composed of six isotopes: ^{78}Kr (0.35%), ^{80}Kr (2.3%), ^{82}Kr (11.6%), ^{83}Kr (11.5%), ^{84}Kr (57.0%), and ^{86}Kr (17.3%) [25]. ^{83}Kr has a nuclear spin of 9/2, a nuclear magnetic moment of -0.97 μm and nuclear quadrupole of $+0.253$ barn [29]. The near infrared spectrum of Kr I was observed in the region of 11870−12700 cm^{-1}. Nevertheless, we missed the region 12018−12039 cm^{-1}, 12594−12601 cm^{-1}, and 12639−12652 cm^{-1} for the reason of fluctuations of our laser. The line profiles for all observed transitions show typical asymmetric line shape, which contain the underlying components of isotope shifts and hyperfine structures.

A. Kr I infrared spectrum

Considering that all lines are initially measured without exact calibration, we used 38 lines of neutral ^{84}Kr from 11883.9039 cm^{-1} to 12699.8662 cm^{-1} given in Table II in Ref.[27] as standard lines. For all spectral lines, their calibration errors are given in parentheses in Tables I, II and III. In this calibration work, we take the approximation between line frequencies of ^{84}Kr in Ref.[27] and the center of gravity of Kr of our measured lines. From the work of Katoh [30], we have learned that the ^{86}Kr-^{84}Kr interval is typically 0.003 cm^{-1}, therefore the error involved in using line frequencies of ^{84}Kr as the center of gravity of neutral Kr is typically less than 0.003 cm^{-1}. Based on the results of Jackson [10, 11] we found that the difference between ^{84}Kr and the center of gravity of neutral Kr range from about 1% to 5% of the ^{86}Kr-^{84}Kr interval.

All lines are listed in Tables I, II, and III. Table I shows 33 classified lines which have been reported in previous works [26, 27]. Table II and Table III list new lines which have not been reported in literatures and can only be observed in the present work. Table II shows 45 lines which can be classified with the known energy levels reported in Refs.[26, 27]. Table III lists 42 new lines which cannot be classified with reported energy levels.

The observed wavelengths and the corresponding wavenumbers are given in the second and third columns of Table I. In the columns 2 and 3 the information on the transitions is provided for air wavelengths (calculated by using formula in Ref.[31]) and wavenumber, respectively. Columns 4 and 5 list the frequencies from NIST atomic database [32] and Ref.[27], respectively. There is a difference of ± 0.01 cm^{-1} between our results and the previous studies. The rest six columns specify the energies (Ref.[27]), terms, and J values of the upper and lower levels. Here, we use J_L coupling notation for all level designations.

All lines in our work are broadened as a result of isotope shift and hyperfine structure. FIG. 1 shows the one of our measured absorption spectra of Kr I of the $4s^24p^5(^2P^o_{1/2})5s[1/2]_1$–$4s^24p^5(^2P^o_{1/2})5p[1/2]_1$ transition at 12072.439 cm^{-1} (8281.054 Å). The underlying components in FIG. 1 illustrate the isotope splitting and hyperfine structure data from Ref.[30]. FIG. 1(a) shows contributions of different isotopes of even mass Kr isotopes. Limited by the spectral resolution, the isotope shifts of Kr I cannot be distinguished in our spectra. FIG. 1(b) shows the same spectrum intensity enhanced in order to emphasize the hyperfine structure of ^{83}Kr. In atoms, hyperfine structure occurs due to the energy of the nuclear magnetic dipole moment in the magnetic field generated by the electrons, and the energy of the nuclear electric quadrupole moment in the electric field gradient due to the distribution of charge within the atom. Once atoms have a non-zero nuclear spin, I, their fine structure levels with a non-zero total angular momentum J will split into sub-levels, which form the hyperfine structures of the spectral lines. A detailed description can be found in Ref.[33]. Based on the selection rules, the $4s^24p^5(^2P^o_{1/2})5s[1/2]_1$-$4s^24p^5(^2P^o_{1/2})5p[1/2]_1$ transition should have seven hyperfine transitions. Only five hyperfine structure components can be seen in our experimental spectrum. Limited by the line width of the Doppler-limited absorption spectrum and the high intensity of the even isotopes, two hyperfine transitions marked by dotted lines in the region of center peak are masked. All hyperfine transitions of odd mass ^{83}Kr are shown in FIG. 1 in the form of (F, F'), where F and F' represent the lower and upper hyperfine quantum numbers.

DOI:10.1063/1674-0068/cjcp1905089

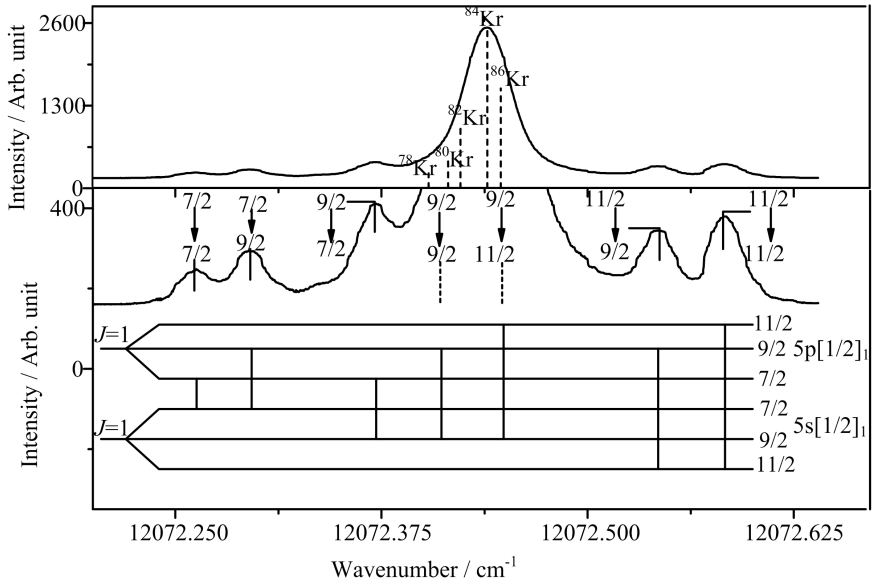

FIG. 1 Spectral lines of Kr I of the $4s^24p^5(^2P^o_{1/2})5s[1/2]-1-4s^24p^5(^2P^o_{1/2})5p[1/2]_1$ transition at 12072.439 cm^{-1} (8281.054 Å). (a) Contributions of different isotopes of even mass Kr isotopes. (b) A higher resolution spectra of odd mass ^{83}Kr I. From left to right, the seven hyperfine transitions of ^{83}Kr I marked in this figure are the (7/2, 7/2), (7/2, 9/2), (9/2, 7/2), (9/2, 9/2), (9/2, 11/2), (11/2, 9/2), and (11/2, 11/2) where (F, F') are the lower and upper level hyperfine quantum numbers respectively. Note that the hyperfine structure of lower state is inverted.

Table II and Table III show our new observed lines. Table II lists 45 new lines that can be classified with the known Kr I energy levels [26, 27]. The second column reports the observed wavelengths and the third lists corresponding observed vacuum wavenumbers. The rest six columns are the energies (Ref.[27]), terms, and J values of the upper and lower levels.

Table III lists 42 new lines which can't be classified with the known energy levels. However, these new lines indicate there are new possible energy levels which haven't been reported in previous studies. The discovery of new levels will help in reducing the number of unclassified lines of Kr I. So, we make further analysis of these new lines.

B. Kr I energy levels

To obtain new energy levels of Kr, a special computer program called "Elements" [34] is employed here. The program can search possible unknown energy levels from unclassified lines via their expected hyperfine patterns based on selection rules and the venerable Ritz combination principle [35]. The method is easily applied for the case where the hyperfine components are well separated. Moreover, if the magnetic dipole constant A, and the electric quadrupole constant, B, which are characteristics of the level, are known, the energy level can be identified.

Search strategies for finding new levels are implemented in the program with menu item "Seek New Level". Before computing, two files should be created: energy level file and wavelength file of Kr I. We assume a certain parity of the new level as odd and take the lowest level of even parity to get the energy of a predicted new odd level. Then we compare the calculated energy levels with the energy levels which are got by other wavenumbers of all other lines within our line list. If the energy obtained in this way coincides with that of predicted level, the wavelengths and even lower levels are listed. Then we repeat the process to get all the possible odd energy levels. If no new odd level is suggested, we try to find a new level having even parity. From one of the line groups of the calculated results, we can get the possible J value of energy level. In addition, it is possible to simulate the hyperfine structure by varying the A_o, B_o, A_u, and B_u values for each of the calculated transitions.

Here we take $4s^24p^5(^2P^o_{1/2})5s[1/2]_1-4s^24p^5(^2P^o_{1/2})5p[1/2]_1$ transition of ^{83}Kr I as an example. After loading the experiment data into the simulation window, we try to varying the A_o, B_o, A_u, and B_u values to make the calculated hyperfine structures fit to the observed structures. From the recorded hyperfine structure of the $4s^24p^5(^2P^o_{1/2})5s[1/2]_1$-$4s^24p^5(^2P^o_{1/2})5p[1/2]_1$ transition of ^{83}Kr I, the J values and hyperfine constants of the involved fine structures levels can be determined. FIG. 2 shows the hyperfine structure of the $4s^24p^5(^2P^o_{1/2})5s[1/2]_1$-$4s^24p^5(^2P^o_{1/2})5p[1/2]_1$ transition in more detail.

Unfortunately, for most of our spectral lines, we can-

DOI:10.1063/1674-0068/cjcp1905089

TABLE I 33 classified lines of Kr I which have been reported in previous work measured in this experiment.

No.	$\sigma_{obs.}$/Å	σ/cm^{-1}			E_L/cm^{-1}	Term	J_L	E_U/cm^{-1}	Term	J_U
	in air	Obs.	NIST	Phys. Scr. (2007)						
1	8412.426(14)	11883.911(20)	11883.909	11883.9039(15)	93123.3409	^{2}[3/2]	2	105007.245	^{2}[3/2]^o	2
2	8332.716(15)	11997.592(21)	11997.57		97085.193	^{2}[1/2]^o	1	109082.770	^{2}[1/2]	1
3	8303.257(17)	12040.157(24)	12040.24	12040.1580(18)	93123.3409	^{2}[3/2]	2	105163.499	^{2}[5/2]^o	2
4	8301.401(14)	12042.850(20)	12042.87	12042.8501(16)	92964.3943	^{2}[3/2]	1	105007.245	^{2}[3/2]^o	2
5	8299.409(19)	12045.740(28)		12045.743(30)	97797.287	^{2}[7/2]^o	4	109843.132	^{2}[9/2]	4
6	8298.107(16)	12047.629(23)	12047.6256	12047.6279(32)	80916.7680	^{2}[3/2]^o	1	92964.3943	^{2}[3/2]	1
7	8281.054(20)	12072.439(29)	12072.4418	12072.4429(30)	85846.7046	^{2}[1/2]^o	1	97919.1468	^{2}[1/2]	1
8	8272.354(13)	12085.135(19)	12085.134	12085.1339(16)	93123.3409	^{2}[3/2]	2	105208.476	^{2}[5/2]^o	3
9	8263.677(10)	12097.825(15)		12097.8224(16)	91168.5150	^{2}[1/2]	1	103266.339	^{2}[3/2]^o	2
10	8263.240(42)	12098.465(62)	12098.4612	12098.4648(32)	85846.7046	^{2}[1/2]^o	1	97945.1164	^{2}[3/2]	2
11	8228.859(18)	12149.013(27)	12148.97	12149.012(30)	97687.779	^{2}[3/2]^o	2	109836.77	^{2}[3/2]	2
12	8222.731(12)	12158.068(18)	12158.13	12158.066(40)	97945.1164	^{2}[3/2]	2	110103.2344	^{2}[3/2]^o	2
13	8218.367(21)	12164.523(31)	12164.47	12164.520(20)	97687.779	^{2}[3/2]^o	2	109852.306	^{2}[5/2]	3
14	8210.061(09)	12176.830(14)	12176.8		97945.1669	^{2}[3/2]	2	110121.9961	^{2}[5/2]^o	2
15	8206.610(13)	12181.951(19)	12181.94	12181.9539(18)	92964.3948	^{2}[3/2]	1	105146.33	^{2}[1/2]^o	1
16	8205.168(12)	12184.092(18)	12184.01		97919.1468	^{2}[1/2]	1	110103.2339	^{2}[3/2]^o	2
17	8195.070(13)	12199.104(19)	12199.105	12199.1042(16)	92964.3943	^{2}[3/2]	1	105163.499	^{2}[5/2]^o	2
18	8192.554(11)	12202.850(17)		12202.8474(18)	97919.1468	^{2}[1/2]	1	110121.9961	^{2}[5/2]^o	2
19	8190.053(52)	12206.577(78)	12206.572	12206.5743(32)	80916.7680	^{2}[3/2]^o	1	93123.3409	^{2}[3/2]	2
20	8144.948(04)	12274.173(06)	12274.16	12274.1748(17)	91168.5150	^{2}[1/2]	1	103442.690	^{2}[5/2]^o	2
21	8132.968(10)	12292.254(15)		12292.252(30)	97945.1664	^{2}[3/2]	2	110237.421	^{2}[5/2]^o	3
22	8112.878(09)	12322.693(14)	12322.6585	12322.6642(34)	79971.7417	^{2}[3/2]^o	2	92294.4012	^{2}[5/2]	3
23	8104.366(34)	12335.636(52)	12335.636	12335.6355(32)	79971.7417	^{2}[3/2]^o	2	92307.3786	^{2}[5/2]	2
24	8103.993(14)	12336.204(21)	12336.16	12336.2063(16)	92294.4012	^{2}[5/2]	3	104630.57	^{2}[7/2]^o	4
25	8059.503(31)	12404.302(48)	12404.2991	12404.3012(32)	85191.6166	^{2}[1/2]^o	0	97595.9153	^{2}[3/2]	1
26	8040.465(17)	12433.672(26)		12433.672(10)	98226.268	^{2}[7/2]^o	3	110659.90	^{2}[9/2]	4
27	8033.528(25)	12444.408(38)	12444.42		98226.268	^{2}[7/2]^o	3	110670.67	^{2}[7/2]	4
28	7993.117(09)	12507.323(14)	12507.32	12507.316(2)	97595.9153	^{2}[3/2]	1	110103.2339	^{2}[3/2]^o	2
29	7982.402(14)	12524.113(22)	12524.107	12524.1125(16)	93123.3409	^{2}[3/2]	2	105647.4536	^{2}[3/2]^o	2
30	7981.776(10)	12525.095(16)	12525.03	12525.0951(20)	93123.3409	^{2}[3/2]	2	105648.434	^{2}[3/2]^o	1
31	7981.148(11)	12526.081(18)		12526.079(20)	92964.3943	^{2}[3/2]	1	110121.9961	^{2}[5/2]^o	2
32	7928.727(10)	12608.897(16)	12609.1006	12609.1004(16)	92307.3786	^{2}[5/2]	2	104916.4792	^{2}[7/2]^o	3
33	7913.498(25)	12633.160(40)	12633.278	12633.2779(16)	91168.5150	^{2}[1/2]	1	103801.7929	^{2}[1/2]^o	1

not observe complete hyperfine patterns or hyperfine splitting of lines. That is to say, we need a new experiment like saturation absorption experiment which can obtain a higher resolution of observed lines. Running the program described above, we get more than 10 new possible even energy levels and odd energy levels for each line. Here we choose 8299.409 Å, 8288.110 Å, 8144.948 Å, 8110.991 Å and 8009.601 Å as an example and the results are shown in FIG. 3. The newly calculated energy level has an energy of 99474.4 cm^{-1}. These lines provide high possibility of being classified by the previously unknown level. Unfortunately, with the line width of the Doppler-limited absorption spectrum, we cannot confirm the new energy values.

Limited by the line width of the Doppler-limited absorption spectrum, the hyperfine structure may be too congested to be identified. Due to the overlapping lines with almost unresolved components, we could not get hyperfine structure positions and obtain the constants, so there may be more than 3 new energy levels theoretically.

IV. CONCLUSION

We investigated 120 lines of Kr I which extend from 11870 cm^{-1} to 12690 cm^{-1}, among them 33 lines classified in previous work, and 87 new first observed lines. With the help of known energy levels, we classified 45 of the new lines. Other 42 new lines were first reported

DOI:10.1063/1674-0068/cjcp1905089

TABLE II 45 new measured lines of Kr I which can be classified with the known energy levels in this experiment.

No.	σ_{obs}/Å (in air)	σ_{obs}/cm^{-1}	E_L/cm^{-1}	Term	J_L	E_U/cm^{-1}	Term	J_U
34	8397.860(55)	11904.523(78)	99646.212	^{2}[3/2]^o	1	111550.5	^{2}[3/2]	1
35	8393.226(52)	11911.096(74)	97945.1664	^{2}[3/2]	2	109856.26	^{2}[5/2]^o	2
36	8384.339(56)	11923.722(80)	99626.882	^{2}[3/2]^o	2	111550.5	^{2}[3/2]	1
37	8300.706(18)	12043.858(26)	98867.429	^{2}[5/2]^o	2	110911.1	^{2}[3/2]	1
38	8293.023(18)	12055.015(26)	97797.287	^{2}[7/2]^o	4	109852.306	^{2}[5/2]	3
39	8287.480(18)	12063.078(26)	97797.287	^{2}[7/2]^o	4	109860.366	^{2}[7/2]	4
40	8278.764(20)	12075.778(29)	97085.193	^{2}[1/2]^o	1	109160.957	^{2}[3/2]	2
41	8267.072(12)	12092.856(17)	97595.9153	^{2}[3/2]	1	109688.7558	^{2}[3/2]^o	1
42	8255.360(26)	12110.013(38)	99079.367	^{2}[5/2]^o	3	111189.50	^{2}[9/2]	4
43	8253.251(13)	12113.108(19)	99079.367	^{2}[5/2]^o	3	111192.66	^{2}[5/2]	3
44	8229.599(18)	12147.920(27)	98855.0698	^{2}[1/2]	0	111002.984	^{2}[1/2]^o	1
45	8229.307(12)	12148.352(18)	97687.779	^{2}[3/2]^o	2	109836.15	^{2}[3/2]	1
46	8224.091(12)	12156.057(17)	97595.9153	^{2}[3/2]	1	109751.9639	^{2}[3/2]^o	2
47	8218.041(18)	12165.006(26)	97687.779	^{2}[3/2]^o	2	109852.76	^{2}[5/2]	2
48	8216.340(16)	12167.524(24)	99646.212	^{2}[3/2]^o	1	111814.039	^{2}[5/2]	2
49	8186.950(12)	12211.204(18)	97085.193	^{2}[1/2]^o	1	109296.1917	^{2}[1/2]	0
50	8182.684(15)	12217.569(22)	98855.0698	^{2}[1/2]	0	111072.5	^{2}[1/2]^o	1
51	8154.005(14)	12260.541(21)	97595.9153	^{2}[3/2]	1	109856.456	^{2}[5/2]^o	2
52	8138.326(13)	12284.162(20)	99079.367	^{2}[5/2]^o	3	111363.5	^{2}[3/2]	2
53	8128.478(08)	12299.044(12)	99079.367	^{2}[5/2]^o	3	111378.38	^{2}[7/2]	3
54	8127.233(07)	12300.928(10)	99079.367	^{2}[5/2]^o	3	111380.299	^{2}[5/2]	3
55	8120.404(11)	12311.272(17)	96771.494	^{2}[1/2]^o	0	109082.770	^{2}[1/2]	1
56	8110.991(28)	12325.560(43)	98867.429	^{2}[5/2]^o	2	111192.99	^{2}[5/2]	2
57	8090.897(151)	12356.170(231)	105964.446	^{2}[3/2]^o	1	112002.419	^{2}[3/2]	2
58	8081.078(11)	12371.185(17)	97919.1468	^{2}[1/2]	1	110290.3165	^{2}[1/2]^o	1
59	8076.520(14)	12378.167(22)	96771.494	^{2}[1/2]^o	0	109149.694	^{2}[3/2]	1
60	8054.379(12)	12412.193(19)	97797.287	^{2}[7/2]^o	4	110209.56	^{2}[5/2]	3
61	8043.068(14)	12429.648(22)	98226.268	^{2}[7/2]^o	3	110656.01	^{2}[3/2]	2
62	8036.865(17)	12439.241(26)	98226.268	^{2}[7/2]^o	3	110665.45	^{2}[5/2]	3
63	8036.636(14)	12439.596(22)	98226.268	^{2}[7/2]^o	3	110665.75	^{2}[5/2]	2
64	8012.926(22)	12476.404(35)	99079.367	^{2}[5/2]^o	3	111555.77	^{2}[5/2]	3
65	8009.601(09)	12481.584(14)	98867.429	^{2}[5/2]^o	2	111348.9	^{2}[5/2]	2
66	8002.677(10)	12492.383(16)	98867.429	^{2}[5/2]^o	2	111359.8	^{2}[3/2]	1
67	7990.813(09)	12510.93(14)	98867.429	^{2}[5/2]^o	2	111378.38	^{2}[7/2]	3
68	7989.573(08)	12512.871(12)	98867.429	^{2}[5/2]^o	2	111380.299	^{2}[5/2]	3
69	7989.020(08)	12513.737(12)	98867.429	^{2}[5/2]^o	2	111381.160	^{2}[5/2]	2
70	7983.918(12)	12521.734(19)	97687.779	^{2}[3/2]^o	2	110209.85	^{2}[5/2]	2
71	7981.349(11)	12525.764(18)	97945.1664	^{2}[3/2]	2	110470.9189	^{2}[7/2]^o	3
72	7965.065(13)	12551.372(21)	97945.1664	^{2}[3/2]	2	110496.7122	^{2}[5/2]^o	2
73	7920.447(10)	12622.078(16)	92294.4012	^{2}[5/2]	3	104916.4792	^{2}[7/2]^o	3
74	7894.457(12)	12663.638(19)	97945.1664	^{2}[3/2]	2	110608.359	^{2}[3/2]^o	2
75	7891.368(12)	12668.586(19)	98226.268	^{2}[7/2]^o	3	110894.8	^{2}[5/2]	3
76	7882.217(32)	12683.297(51)	98867.429	^{2}[5/2]^o	2	111550.5	^{2}[3/2]	1
77	7881.753(11)	12684.042(18)	92964.3943	^{2}[3/2]	1	105648.434	^{2}[3/2]^o	1
78	7878.532(09)	12689.229(15)	97919.1468	^{2}[1/2]	1	110/608.359	^{2}[3/2]^o	2

DOI:10.1063/1674-0068/cjcp1905089

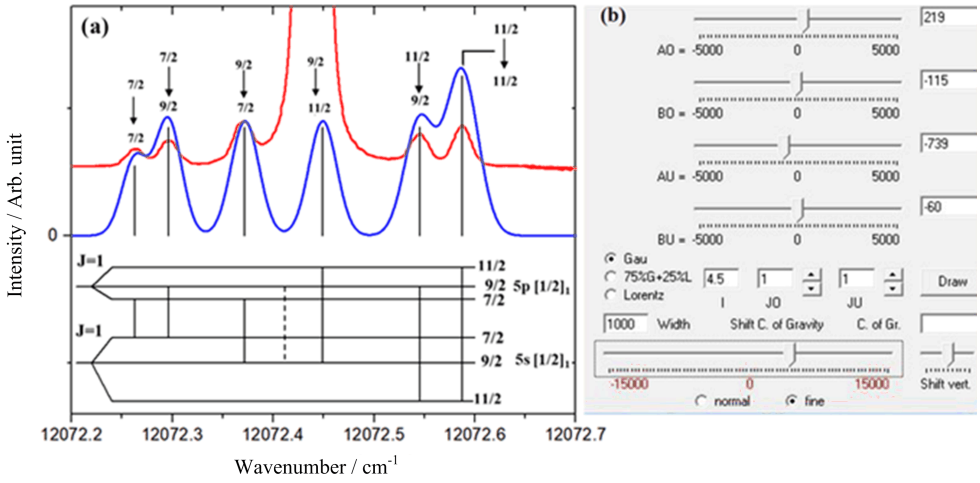

FIG. 2 The simulation window of the program "Elements" showing the $4s^24p^5(^2P^o{}_{1/2})5s[1/2]_1$–$4s^24p^5(^2P^o{}_{1/2})5p[1/2]_1$ transition at 12072.439 cm^{-1} (8281.054 Å). (a) The hyperfine information of the selected spectral line. The red line is the observed spectral line of ^{83}Kr I, the blue line is the calculated hyperfine of ^{83}Kr I. (b) The operation-window. The observed spectral profile can be loaded into the simulation window and compared with the calculated hyperfine pattern by varying four buttons of the A_o, B_o, A_u, and B_u, which are hyperfine constants of the upper levels and lower levels, respectively.

TABLE III 42 new measured lines of Kr I which can't be classified with reported energy levels in this experiment.

No.	σ_{obs}/cm^{-1}	No.	σ_{obs}/cm^{-1}
79	11873.061(34)	101	12473.037(26)
80	11878.737(24)	102	12478.350(44)
81	11899.107(61)	103	12479.299(39)
82	11906.124(42)	104	12479.634(36)
83	11906.279(19)	105	12492.647(20)
84	11914.806(82)	106	12522.238(16)
85	11917.753(21)	107	12566.599(37)
86	11926.455(33)	108	12568.332(24)
87	11951.021(57)	109	12572.437(12)
88	11978.077(26)	110	12572.837(13)
89	11978.641(21)	111	12574.499(33)
90	11992.420(18)	112	12574.797(12)
91	12062.161(19)	113	12580.868(21)
92	12107.519(25)	114	12588.554(18)
93	12116.832(40)	115	12615.446(56)
94	12167.824(48)	116	12617.335(158)
95	12238.434(11)	117	12668.439(17)
96	12328.756(49)	118	12677.871(16)
97	12330.140(51)	119	12678.851(17)
98	12332.338(148)	120	12685.09(75)

in the present work. By applying a classification computer program to these new lines, we derived some new possible energy levels. Limited by the Doppler broadening, we should make further effort to confirm these energy level values. Many spectral lines still remain unclassified and further investigation should be carried out.

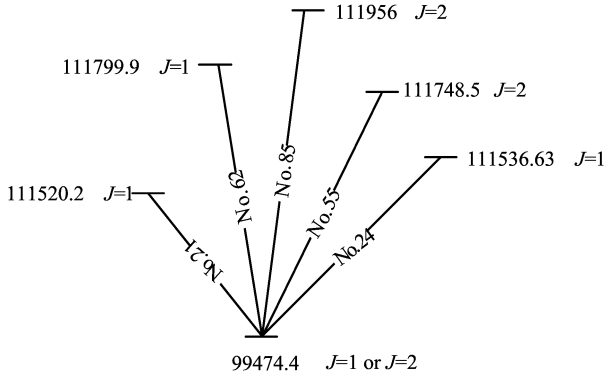

FIG. 3 New energy level at 99474.4 cm^{-1}, explaining the five new excitation wavelengths (8299.409, 8288.110, 8144.948, 8110.991, and 8009.601 Å).

V. ACKNOWLEDGMENTS

This work was supported by the National Natural Science Foundation of China (No.11674096). The authors would like to thank Prof. L. Windholz at Graz University of Technology, for making the program "Elements" accessible.

[1] H. L. Dinerstein, Astrophys. J. **550**, L223 (2001).
[2] J. A. Cardelli and D. M. Meyer, Astrophys. J. **477**, L57 (1997).
[3] W. F. Meggers, T. L. de Bruin, and C. J. Humphreys, J. Res. Natl. Bur. Stand. **3**, 129 (1929).
[4] W. F. Meggers, T. L. de Bruin, and C. J. Humphreys, J. Res. Natl. Bur. Stand. **7**, 643 (1931).

DOI:10.1063/1674-0068/cjcp1905089

[5] W. F. Meggers and C. J. Humphreys, J. Res. Natl. Bur. Stand. **10**, 427 (1933).
[6] W. R. Sittner and E. R. Peck, J. Opt. Soc. Am. **39**, 474 (1949)
[7] C. J. Humphreys and H. J. Kostkowski, J. Res. Natl. Bur Stand. **49**, 84 (1952).
[8] C. E. Moore, Natl. Bur. Stand. Cric. 467 (1971).
[9] V. Kaufman and C. J. Humphreys, J. Opt. Soc. Am. **59**, 28 (1969).
[10] D. A. Jackson, J. Opt. Soc. Am. **69**, 505 (1979).
[11] D. A. Jackson, J. Opt. Soc. Am. **70**, 1139 (1980).
[12] T. Trickl, M. J. J. Vrakking, E. Cromwell, Y. T. Lee, and A. H. Kung, Phys. Rev. A **39**, 2948 (1989).
[13] J. Sugar and A. Musgrove, J. Phys. Chcm. Ref. Data **20**, 859 (1991).
[14] C. J. Sansonetti, M. M. Blackwell, and E. B. Saloman, Phys. Scr. **T100**, 120 (2002).
[15] C. J. Humphreys, E. Paul, Jr., R. D. Cowan, and K. L. Andrew, J. Opt. Soc. Am. **57**, 855 (1967).
[16] F. B. Dunning and R. F. Stebbings, Phys. Rev. A **9**, 2378 (1974).
[17] X. Husson and J. P. Grandin, J. Phys. B **12**, 3649 (1979).
[18] M. Aymar, O. Robaux, and C. Thomas, J. Phys. B **14**, 4255 (1981).
[19] E. Audouard, P. Laporte, J. L. Subtil, N. Damany, and M. Pellarin, Phys. Rev. A **41**, 6032 (1990).
[20] M. Bounakhla, J. P. Lemoigne, J. P. Grandin, X. Husson, H. Kucal, and M. Aymar, J. Phys. B **26**, 345 (1993).
[21] K. Ito, H. Masuda, Y. Morioka, and K. Ueda, Phys. Rev. A **47**, 1187 (1993).
[22] V. Kaufman, J. Res. Natl. Inst. Stand. Technol. **98**, 717 (1993).
[23] M. Ahmed, M. A. Zia, M. A. Baig, and B. Suleman, J. Phys. B **30**, 2155 (1997).
[24] A. P. Mishra, R. J. Kshirsagar, V. P. Bellary, and T. K. Balasubramanian, J. Quant. Spectrosc. Radiat. Transf. **67**, 1 (2000).
[25] F. Brandi, W. Hogervorst, and W. Ubachs, J. Phys. B **35**, 1071 (2002).
[26] E. B. Saloman, J. Phys. Chem. Ref. Data **36**, 1 (2007).
[27] C. J. Sansonetti and M. B. Greene, Phys. Scr. **75**, 577 (2007).
[28] X. Ni, L. H. Deng, and H. L. Wang, J. Quant. Spectrosc. Radiat. Transf. **196**, 168 (2017).
[29] R. D. Cowan, *The Theory of Atomic Structure and Spectra*, Berkeley, CA: University of California Press, and Cowan programs RCN, RCN2, and RCG (1981).
[30] K. Katoh, N. Nishimiya, and M. Suzuki, The Academic Reports **28**, 1 (2005).
[31] K. P. Birch and M. J. Downs, Metrologia **30**, 3 (1993)
[32] A. Kramida, Yu. Ralchenko, J. Reader, and NIST ASD Team. *NIST Atomic Spectra Database* (ver. 5.3), Online available: http://physics.nist.gov/asd (2017, October 10). National Institute of Standards and Technology, Gaithersburg, MD. (2015).
[33] L. H. Deng, X. Y. Li, Y. Y. Zhu, and Y. Q. Chen, J. Quant. Spectrosc. Radiat. Transf. **161**, 6 (2015).
[34] (a) L. Windholz and G. H. Guthöhrlein, Phys. Scr. **105**, 55 (2003)
(b) L. Windholz, Phys. Scr. **91**, 114003 (2016).
[35] W. Ritz, Astrophys. J. **28**, 237 (1908).

DOI:10.1063/1674-0068/cjcp1905089